



# Evaluating the soil evaporation loss rate in a gravel-sand mulching environment based on stable isotopes data

YANG Ye<sup>1,2</sup>, ZHANG Mingjun<sup>1,2\*</sup>, ZHANG Yu<sup>1,2</sup>, WANG Shengjie<sup>1,2</sup>, WANG Jiaxin<sup>1,2</sup>

<sup>1</sup> College of Geography and Environmental Science, Northwest Normal University, Lanzhou 730070, China;

<sup>2</sup> Key Laboratory of Resource Environment and Sustainable Development of Oasis, Lanzhou 730070, China

**Abstract:** In order to cope with drought and water shortages, the working people in the arid areas of Northwest China have developed a drought-resistant planting method, namely, gravel-sand mulching, after long-term agricultural practices. To understand the effects of gravel-sand mulching on soil water evaporation, we selected Baifeng peach (*Amygdalus persica* L.) orchards in Northwest China as the experimental field in 2021. Based on continuously collected soil water stable isotopes data, we evaluated the soil evaporation loss rate in a gravel-sand mulching environment using the line-conditioned excess (lc-excess) coupled Rayleigh fractionation model and Craig-Gordon model. The results show that the average soil water content in the plots with gravel-sand mulching is 1.86% higher than that without gravel-sand mulching. The monthly variation of the soil water content is smaller in the plots with gravel-sand mulching than that without gravel-sand mulching. Moreover, the average lc-excess value in the plots without gravel-sand mulching is smaller. In addition, the soil evaporation loss rate in the plots with gravel-sand mulching is lower than that in the plots without gravel-sand mulching. The lc-excess value was negative for both the plots with and without gravel-sand mulching, and it has good correlation with relative humidity, average temperature, input water content, and soil water content. The effect of gravel-sand mulching on soil evaporation is most prominent in August. Compared with the evaporation data of similar environments in the literature, the lc-excess coupled Rayleigh fractionation model is better. Stable isotopes evidence shows that gravel-sand mulching can effectively reduce soil water evaporation, which provides a theoretical basis for agricultural water management and optimization of water-saving methods in arid areas.

**Keywords:** soil evaporation loss rate; gravel-sand mulching; stable isotopes; line-conditioned excess coupled Rayleigh fractionation model; Craig-Gordon model

**Citation:** YANG Ye, ZHANG Mingjun, ZHANG Yu, WANG Shengjie, WANG Jiaxin. 2022. Evaluating the soil evaporation loss rate in a gravel-sand mulching environment based on stable isotopes data. Journal of Arid Land, 14(8): 925–939. <https://doi.org/10.1007/s40333-022-0101-1>

## 1 Introduction

China's total freshwater resources account for 6% of the world's total, and its per capita annual water resources account for only 28% of the world's total. The amount of water resources per hectare of arable land in China is  $2.1 \times 10^4 \text{ m}^3$ , accounting for 50% of the world average (Kang, 2019; Yuan et al., 2019). The shortage of water resources has become a severe challenge to

\*Corresponding author: ZHANG Mingjun (E-mail: mjzhang2004@163.com)

Received 2022-05-24; revised 2022-07-19; accepted 2022-08-04

© Xinjiang Institute of Ecology and Geography, Chinese Academy of Sciences, Science Press and Springer-Verlag GmbH Germany, part of Springer Nature 2022

China's agricultural development. In Northwest China, gravel-sand mulching emerged as a characteristic agricultural technology in agricultural activities. It is a drought-resistant planting method developed by people working in the arid environments after long-term farming practices adapted to drought and water shortage. Gravel-sand mulching refers to covering the soil surface with gravel or sand, thereby inhibiting soil water evaporation (Zhao et al., 2017) and increasing soil water storage (Poesen et al., 1997). Evaporation is the main way of soil water consumption and the main output of the regional water cycle (Che et al., 2020). It is also an important factor causing soil water loss and drought. Therefore, reasonable reduction of soil water evaporation can effectively increase the total crop water supply and comprehensively reduce the impact of water storage on crop growth.

The traditional evaporation assessment mostly adopts micro lysimeter, soil heat pulse, chamber, micro-Bowen ratio energy balance analysis, and eddy covariance (Kool et al., 2014). However, these methods are time-consuming and expensive when obtaining the long-term evaporation data. Although modeling is useful for estimating the soil evaporation loss rate over a relatively long period, few models can estimate evaporation under the canopy; even if they can, they tend to overestimate the amount of soil evaporation loss rate, which needs to be verified by long-term field monitoring (Xiang et al., 2021).

The stable isotopes ratio of water (i.e.,  $^2\text{H}/^1\text{H}$  and  $^{18}\text{O}/^{16}\text{O}$ ) is a good tracer for studying water movement and flux (Kool et al., 2014; Sprenger et al., 2017). Evaporation of the soil surface is the main cause of soil water stable isotopes enrichment, and the degree of evaporation depends on the time of surface exposure as well as other soil and climatic conditions (Hasselquist et al., 2018; Ducklert et al., 2019). To date, a lot of study has been done to estimate the soil evaporation loss rate under experimental and field conditions through the isotopic composition of water in shallow soils (Barnes and Allison, 1984; Hsieh et al., 1998; Sprenger et al., 2017; Al-Oqaili et al., 2020; Mahindawansha et al., 2020). As a supplement to the traditional method, the main advantage of the method based on stable isotope is that the estimates correspond to a relatively long period (such as days and months) before soil sampling, and it does not require continuous field observations (Barnes and Allison, 1984). In the past, the classical Craig-Gordon model was usually used to evaluate the evaporation loss of soil or lake by the stable isotope method (Craig and Gordon, 1965; Gibson et al., 2016; Sprenger et al., 2017; Che et al., 2020; Mahindawansha et al., 2020). Utilizing the measured values of  $\delta^{18}\text{O}$  and  $\delta^2\text{H}$  in water, this model can be used to calculate the soil evaporation loss rate. However, the soil evaporation loss rate calculated based on  $\delta^{18}\text{O}$  and  $\delta^2\text{H}$  is usually different in practical applications (Sprenger et al., 2017; Hu et al., 2018; Mahindawansha et al., 2020). To make the calculation results more accurate, we used the dual-isotope systems method (line-conditioned excess (lc-excess) coupled Rayleigh fractionation model) and the traditional single-isotope systems method (Craig-Gordon model) to quantify the soil evaporation loss rate in this study.

Baifeng peach (*Amygdalus persica* L.) is widely planted in Gansu Province of China, and the economic benefits are considerable. In the relatively harsh natural environment, the healthy and sustainable development of economic forests is particularly important. Therefore, the evaluation of soil evaporation loss rate in the gravel-sand mulching environment of Baifeng peach orchards can provide data support for agricultural production activities, which is of great significance for the efficient use of limited water resources to maintain the sustainable and healthy development of fruit trees and support water management in orchards. In order to determine the impact of gravel-sand mulching on soil evaporation, we monitored the changes of soil water content and soil water stable isotope values in the plots with and without gravel-sand mulching during the peach tree growing season (from April to October) in 2021. The objectives of this study were to: (1) estimate the effect of gravel-sand mulching on the soil water content; (2) assess the soil evaporation loss rate in the gravel-sand mulching environment; and (3) evaluate the reliability of the soil evaporation loss rate calculations.

## 2 Materials and methods

### 2.1 Study area

The experimental field is located in the western Loess Plateau of China (36°08'N, 103°40'E) and belongs to the arid and semi-arid climate zone (Dang, 2004). The average annual precipitation is 312.9 mm, the annual average temperature is 7.4°C, the potential evaporation is 1676 mm, the sunshine duration is 2447 h, and the frost-free period is 180 d (Chen et al., 2013). The natural soil is mainly dark gray calcareous soil and typical gray calcareous soil, which is barren and poor in soil and water conservation. The arable soil is mainly anthropogenic, which is the result of long-term cultivation, irrigation, and fertilization. The experimental field covers an area of 666.7 m<sup>2</sup>, with irrigation canals in the north and east, other farmlands in the south, roads in the west, and there are two ridges in the field (Fig. 1).

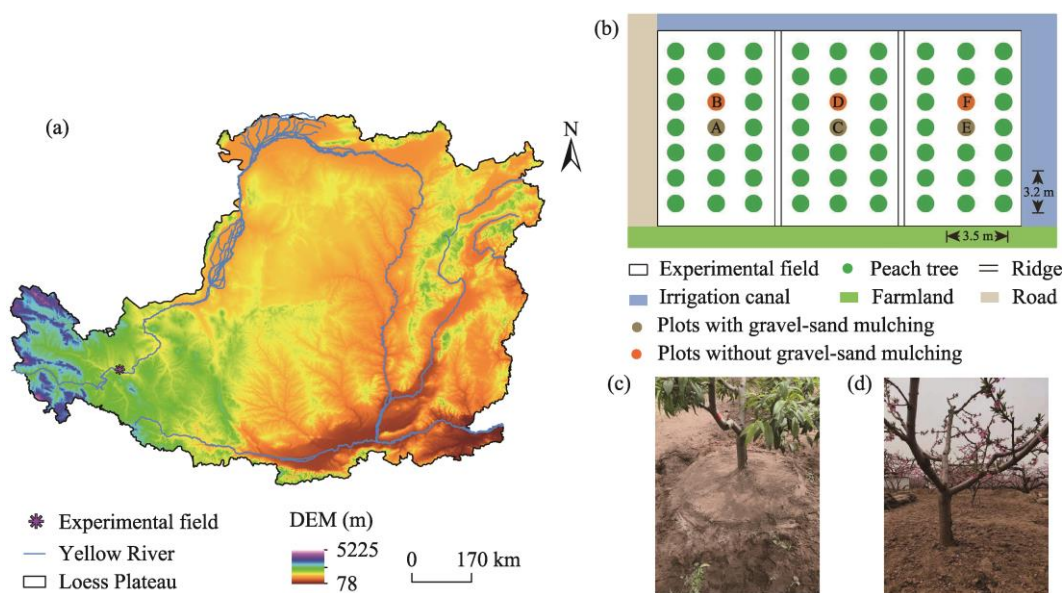


**Fig. 1** Location of the experimental field in the Loess Plateau (a), overview of the experimental field (b), and photographs of the plots with gravel-sand mulching (c) and without gravel-sand mulching (d). DEM, digital elevation model; A, C, and E are the plots with gravel-sand mulching; B, D, and F are the plots without gravel-sand mulching.

### 2.2 Sampling and measurement of soil

We selected six well-growing peach trees (Fig. 1b) in the experimental field, distributed on both sides of the two ridges; all the trees are Baifeng peach. In Figure 1b, trees marked with A, C, and E are covered with 5.0-cm thick sand and gravel after soil sampling in May 2021, and trees marked with B, D, and F are the plots without gravel-sand mulching. The radius of coverage area is 0.8 m, and the particle size of sand and gravel is less than 5.0 mm. The coverage measures used in this study are based on the experiences of local farmers. Soil samples were collected at a distance of 0.8 m from the peach tree. After manually excavating the soil profile at 0.5 m, a soil drill with a depth of 1.0 m was used for deep sampling. The sampling interval is 0.1 m, and the total sampling depth is 1.5 m. We collected 4 parallel samples from each layer of soil, and a total of 2688 samples were collected. A part of the soil samples was placed into aluminum boxes to determine the soil water content. The other part was sealed in a glass bottle and then frozen and stored until experimental stable isotope analysis was carried out.

All the collected samples were analyzed in the stable isotopes laboratory of the College of Geography and Environmental Science, Northwest Normal University. Water in the soil was extracted by an automatic vacuum condensation extraction system (LI-2200, BeiJingJianLing,

Beijing, China). The vacuum degree was controlled below 1 Pa/s, the heating temperature was 105°C, and the extraction time was 3 h. After extraction, we randomly selected some samples and weighed them to ensure that the extraction efficiency was greater than 98%. The isotopic composition of the extracted soil water and precipitation was determined by a liquid water stable isotope analyzer (T-LWIA-45-EP, Los Gatos Research, California, USA). The measured  $\delta^{18}\text{O}$  and  $\delta^2\text{H}$  are expressed in thousandths, which are the difference relative to the Vienna Standard Mean Ocean Water. The equation can be expressed as follows:

$$\delta = \left( \frac{R_{\text{sample}}}{R_{\text{standard}}} - 1 \right) \times 1000\text{‰}, \quad (1)$$

where  $\delta$  is the isotopic composition ( $\delta^2\text{H}$  or  $\delta^{18}\text{O}$ ) in the water sample;  $R_{\text{sample}}$  is the ratio of the heavy isotope to the light isotope in the water sample, i.e.,  $^2\text{H}/^1\text{H}$  and  $^{18}\text{O}/^{16}\text{O}$ ; and  $R_{\text{standard}}$  is the isotope ratio in the Vienna Standard Mean Ocean Water. The standard error of measurement is  $\pm 1.0\text{‰}$  for  $\delta^2\text{H}$  and  $\pm 0.3\text{‰}$  for  $\delta^{18}\text{O}$ . Organic substances, such as methanol, ethanol, and other biovolatile compounds, may be mixed in the process of extracting soil water by low-temperature vacuum distillation, which will lead to large isotope differences in the process of laser analysis. To eliminate the pollution caused by organic substances, we used the spectral analysis software (Version 3.1.0.9, Los Gatos Research, California, USA) to establish the correction curve, and corrected the isotopes of soil water data based on the index of the measured absorption spectrum.

The soil water content was calculated by the drying and weighing method. The wet soil was weighed with an electronic balance, baked for approximately 24 h in a constant temperature oven ( $105^\circ\text{C} \pm 2^\circ\text{C}$ ), dried to constant weight, and then weighed. The calculation formula is as follows:

$$\text{SWC} = \left( \frac{W_1 - W_2}{W_2 - W_0} \right) \times 100\%, \quad (2)$$

where SWC is the soil water content (%);  $W_1$  is the weight of wet soil in the aluminum box before drying (g);  $W_2$  is the weight of the aluminum box with dry soil after drying (g); and  $W_0$  is the weight of the empty aluminum box (g).

### 2.3 Meteorological data

The meteorological data during the sampling period were recorded using the automatic weather station in the meteorological field of Northwest Normal University (WatchDog 2000, Spectrum Technologies, Chicago, USA), including air temperature and relative humidity. Precipitation stable isotopes data are derived from precipitation collected in the meteorological field from 2019 to 2021. The rain gauge was located next to the automatic weather station and was used to collect rainfall generated by each rainfall event from 2019 to 2021.

### 2.4 Determination of the soil evaporation loss rate

#### 2.4.1 Line-conditioned excess (lc-excess) coupled Rayleigh fractionation model

In this study, we assumed that the fractionation of hydrogen and oxygen stable isotopes in the process of soil water evaporation conforms to the Rayleigh fractionation model (Clark and Fritz, 2013). The soil evaporation loss rate ( $f$ ; %) can be calculated as follows:

$$R_s = R_p (1 - f)^{(\alpha-1)}, \quad (3)$$

where  $R_s$  and  $R_p$  represent the ratio of  $^2\text{H}/^1\text{H}$  (or  $^{18}\text{O}/^{16}\text{O}$ ) to soil water and soil water source, respectively; and  $\alpha$  represents the fractionation factor.

Replace  $R_s$  and  $R_p$  in Equation 3 with  $\delta_s$  and  $\delta_p$ , respectively, we can obtain Equation 4:

$$\delta_p = (\delta_s + 1000)(1 - f)^{(1-\alpha)} - 1000, \quad (4)$$

where  $\delta_s$  (‰) and  $\delta_p$  (‰) are the stable isotopes values of soil water and soil water source, respectively.

$$\alpha = (1 - \varepsilon_k \times 10^{-3}) / \alpha^+, \quad (5)$$

where  $\alpha^+$  is the equilibrium fractionation factor and  $\varepsilon_k$  is the dynamic fractionation factor (Horita et al., 2008).

Landwehr and Coplen (2006) proposed lc-excess value to evaluate whether there is an isotopes shift between soil water and soil water source. In this study, lc-excess value represents the deviation degree of the isotopes value concerning the input water line. The equation of lc-excess value can be expressed as:

$$\text{lc-excess} = \delta^2\text{H} - (a \times \delta^{18}\text{O} + b), \quad (6)$$

where  $a$  and  $b$  are the slope and intercept of the input water line, respectively.

The physical meaning of lc-excess is expressed as the degree of deviation of the isotopes value in the sample from the input water line, indicating the non-equilibrium dynamic fractionation process caused by evaporation. Therefore, Formula 7 can be obtained:

$$\text{lc-excess} = (\delta^2\text{H}_s + 1000) \left( (1-f)^{(1-\alpha_{2\text{H}})} \right) - 1000 - a \left( (\delta^{18}\text{O}_s + 1000) \left( (1-f)^{(1-\alpha_{18\text{O}})} \right) - 1000 \right) - b, \quad (7)$$

where  $\delta^2\text{H}_s$  and  $\delta^{18}\text{O}_s$  represent stable isotopes of soil water.

#### 2.4.2 Craig-Gordon model

Based on the principle of isotopes mass balance, we used the Craig-Gordon model to calculate the soil evaporation loss rate in an open liquid-vapor isotopes system (Gonfiantini, 1986; Sprenger et al., 2017). The formula of soil evaporation loss rate ( $f$ , %) is as follows:

$$f = 1 - \left[ \frac{(\delta_s - \delta^*)}{(\delta_p - \delta^*)} \right]^m, \quad (8)$$

where  $\delta^*$  is the limiting factor for isotopes enrichment (Gonfiantini, 1986). The formula is as follows (Gibson et al., 2014):

$$\delta^* = \frac{h\delta_A - \varepsilon_k + \varepsilon^+ / \alpha^+}{h - 10^{-3}(\varepsilon_k + \varepsilon^+ / \alpha^+)}, \quad (9)$$

$$m = \frac{h - 10^{-3}(\varepsilon_k + \varepsilon^+ / \alpha^+)}{1 - h + 10^{-3}\varepsilon_k}, \quad (10)$$

where  $h$  is the relative humidity in the air;  $\delta_A$  is the isotopes value in the surrounding air;  $\varepsilon^+$  is the equilibrium fractionation coefficient (Gibson et al., 2008); and  $m$  is the enrichment slope.  $\delta_A$  can be calculated as follows:

$$\delta_A = \frac{\delta_p - \varepsilon^+}{\alpha^+}. \quad (11)$$

We calculated  $\alpha^+$  and  $\varepsilon^+$  according to Horita et al. (1994):

$$10^3 \ln [\alpha_{(2\text{H})}^+] = \frac{1158.8T^3}{10^9} - \frac{1620.1T^2}{10^6} + \frac{794.84T}{10^3} - 161.04 + \frac{2.9992 \times 10^9}{T^3}, \quad (12)$$

$$10^3 \ln [\alpha_{(18\text{O})}^+] = -7.685 + \frac{6.7123 \times 10^3}{T} - \frac{1.6664 \times 10^6}{T^2} + \frac{0.3504 \times 10^9}{T^3}, \quad (13)$$

$$\varepsilon^+ = (\alpha^+ - 1) \times 1000, \quad (14)$$

where  $T$  is the temperature (K).  $\varepsilon_k$  is the dynamic fractionation factor, and the formulae for  $\delta^2\text{H}$  and  $\delta^{18}\text{O}$  are as follows (Merlivat, 1978):

$$\varepsilon_{k(2\text{H})} = n \times (1-h) \times (1-0.9755), \quad (15)$$

$$\varepsilon_{k(18\text{O})} = n \times (1-h) \times (1-0.9723), \quad (16)$$

where  $n$  is the aerodynamic parameter of the liquid-air interface during evaporation. Generally, it is 0.50 for saturated soil and 1.00 for dry soil (Benettin et al., 2018). Affected by precipitation

infiltration and soil evaporation, the topsoil is often in the process of alternating dry and wet conditions. Therefore, we set 0.75 as the average value of parameter  $n$  in this study, representing the average dry-wet condition of the soil (Mahindawansha et al., 2020).

The slope of the local evaporation line ( $S_{SEL}$ ) is calculated as (Gonfiantini, 1986):

$$S_{SEL} = \left[ \frac{h(\delta_o - \delta_A) - (1 + \delta_o \times 0.001)(\varepsilon_k + \varepsilon^+ / \alpha^+)}{1 - h + \varepsilon_k \times 0.001} \right]_{-2}^{18}, \quad (17)$$

where  $\delta_o$  is the isotopes value of the multi-year average precipitation.

The intercept ( $I_{SEL}$ ) of the soil evaporation line was calculated based on the isotopes of soil water ( $\delta^2\text{H}_s$  and  $\delta^{18}\text{O}_s$ ):

$$I_{SEL} = \delta^2\text{H}_s - S_{SEL} \times \delta^{18}\text{O}_s. \quad (18)$$

The isotopes of the soil water source ( $\delta^{18}\text{O}_{\text{intersect}}$  and  $\delta^2\text{H}_{\text{intersect}}$ ) is the intersection of the soil evaporation line and the input water line (Javaux et al., 2016). The formula is as follows:

$$\delta^{18}\text{O}_{\text{intersect}} = \frac{I_{SEL} - b}{a - S_{SEL}}. \quad (19)$$

$$\delta^2\text{H}_{\text{intersect}} = a\delta^{18}\text{O}_{\text{intersect}} + b. \quad (20)$$

## 2.5 Statistical analysis

For a given mean value and standard error, we used Student's  $t$  test to analyze the difference between the two mean values with unequal variances:

$$t = \frac{x - y}{\sqrt{\sigma x^2 + \sigma y^2}}, \quad (21)$$

where  $x$  and  $y$  are the two mean values; and  $\sigma x$  and  $\sigma y$  are their standard errors, respectively. The statistically significant difference was indicated by  $t > 1.96$  ( $P < 0.05$ ).

## 3 Results

### 3.1 Soil water content

In terms of temporal variation, the soil water content of the plots without gravel-sand mulching changed significantly between different months (Fig. 2). The variation range was between 0.17%/month and 3.00%/month. The average soil water content was higher in May and September, and relatively low in October, which was closely related to the water input during the sampling interval. The correlation coefficient between the soil water content and input water content was 0.75 ( $P < 0.01$ ), with a positive correlation (Table 1). The monthly variation range of the soil water content in the plots with gravel-sand mulching was 0.86%/month to 2.94%/month, which was smaller than that in the plots without gravel-sand mulching. The maximum and minimum values of the average soil water content appeared in September and October, respectively. In terms of spatial variation, the soil water content at the soil depth of 0–30 cm was the most significant ( $P > 0.05$ ), that at the soil depth of 30–150 cm was relatively stable, and that at the soil depth of 100–150 cm was low. In short, the soil water content of the plots with gravel-sand mulching was higher than that of the plots without gravel-sand mulching both in time and space, indicating that gravel-sand mulching can indeed play a role in soil and water conservation.

### 3.2 Stable isotopes of soil water

During the whole sampling period, the average  $\delta^2\text{H}$  and  $\delta^{18}\text{O}$  in the soil water source were  $-84.99\text{‰}$  and  $-12.21\text{‰}$ , respectively; the average  $\delta^2\text{H}$  and  $\delta^{18}\text{O}$  in the plots without gravel-sand

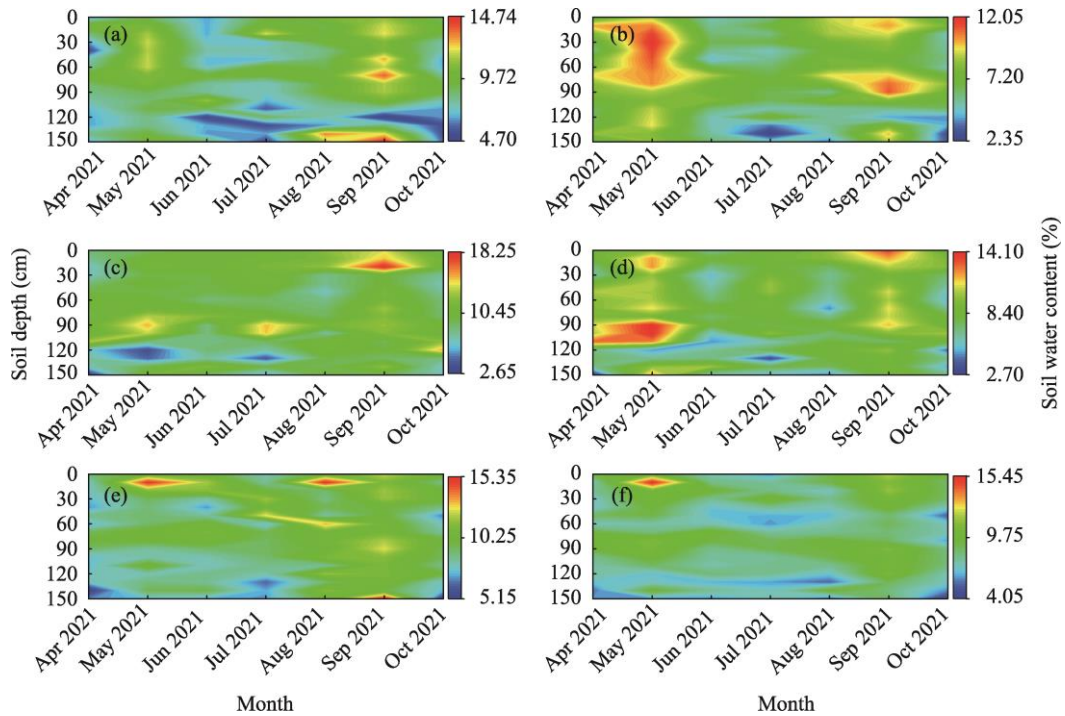


**Fig. 2** Temporal and spatial variation of the soil water content. (a, c, and e), the plots with gravel-sand mulching; (b, d, and f), the plots without gravel-sand mulching.

**Table 1** Correlation analysis between the soil evaporation loss rate and other factors

Factor	$f(^{18}\text{O})$	$f(^2\text{H})$	$f(\text{lc-excess})$	RH	T	IW	SWC	Lc-excess	CW
$f(^{18}\text{O})$	1.00								
$f(^2\text{H})$	0.97**	1.00							
$f(\text{lc-excess})$	0.98**	0.98**	1.00						
RH	-0.71*	-0.66*	-0.76*	1.00					
T	0.55*	0.50*	0.61*	-0.92**	1.00				
IW	-0.44*	-0.54*	-0.54*	-	-	1.00			
SWC	-0.73**	-0.70**	-0.76**	0.29**	-0.27**	0.75**	1.00		
Lc-excess	-0.56**	-0.48**	-0.62**	0.50**	-0.48**	0.61**	0.87**	1.00	
CW	0.60**	0.77**	0.72**	-	-	-	-	-	1.00

Note:  $f(^{18}\text{O})$ , the soil evaporation loss rate calculated by  $\delta^{18}\text{O}$  using Craig-Gordon model;  $f(^2\text{H})$ , the soil evaporation loss rate calculated by  $\delta^2\text{H}$  using Craig-Gordon model;  $f(\text{lc-excess})$ , the soil evaporation loss rate calculated by line-conditioned excess coupled Rayleigh fractionation model; RH, relative humidity; T, average temperature; IW, input water content; SWC, soil water content; Lc-excess, line-conditioned excess value; CW, crown width. \*,  $P < 0.05$ ; \*\*,  $P < 0.01$ ; -, no data.

mulching were  $-70.47\text{‰}$  and  $-9.46\text{‰}$ , respectively; and the average  $\delta^2\text{H}$  and  $\delta^{18}\text{O}$  in the plots with gravel-sand mulching were  $-75.13\text{‰}$  and  $-10.49\text{‰}$ , respectively (Fig. 3). Since the water input of these plots are derived from more than the atmospheric precipitation, there will be irrigation in the early stage of plant growth, and we regard the irrigation water as strong "precipitation" and jointly fit the water line equation, which is called the input water line. Considering the input of precipitation and irrigation water in the later stage, we fit the input water line of each month and calculated the soil evaporation line of each month. The stable isotopes values of soil water in each month were lower than that of the input water line (Fig. 4), and the slope and intercept of the soil water evaporation line were also smaller than those of the input water line, indicating that there was no other water input in these plots and that the soil water was affected by evaporation. Regardless of whether the plots are mulched with gravel and sand, the stable isotopes values of soil water first decreased and then stabilized. The stable isotopes values

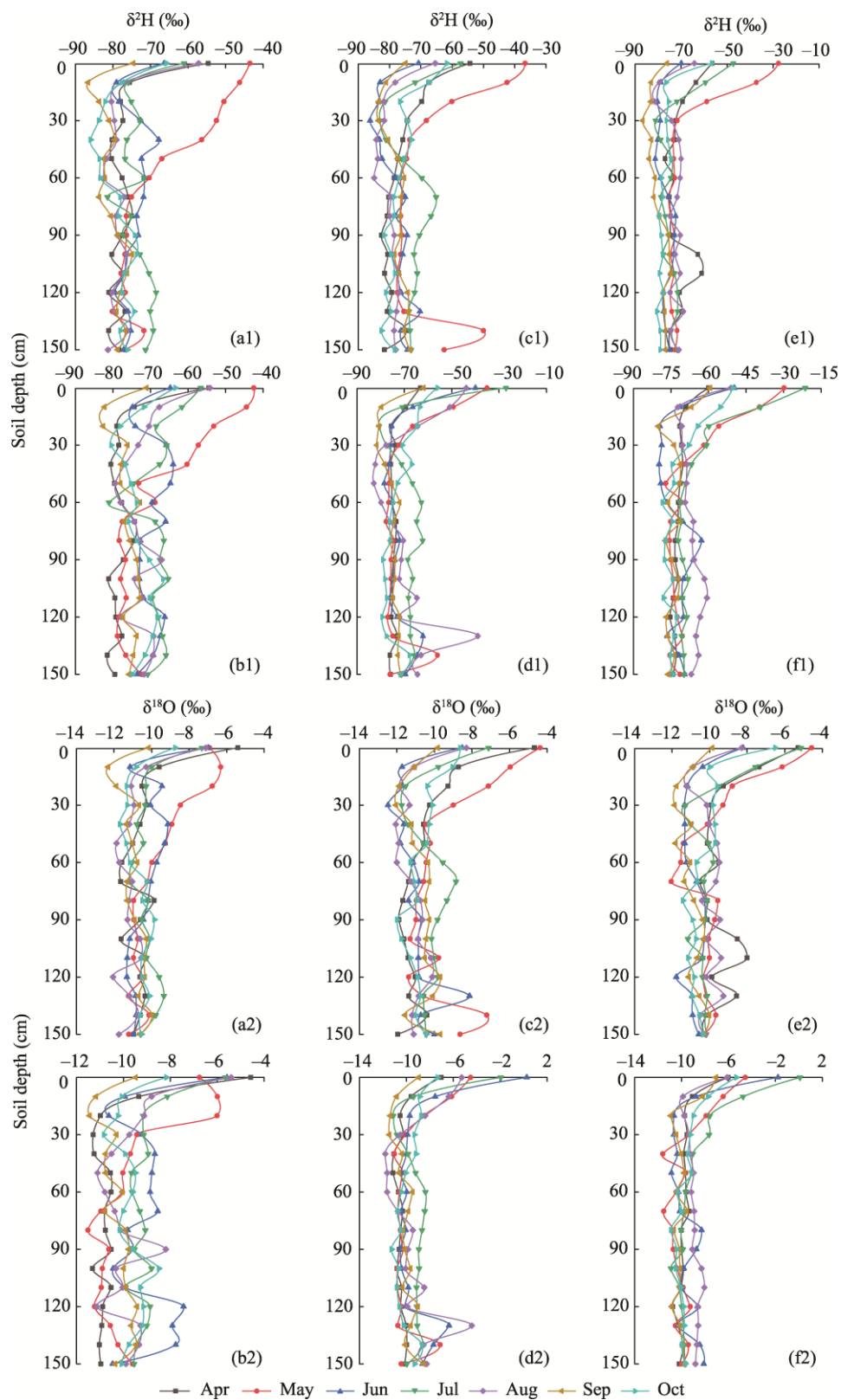


**Fig. 3** Temporal and spatial changes of the stable isotopes values of soil water. (a1–f1) represent  $\delta^2\text{H}$  and (a2–f2) represent  $\delta^{18}\text{O}$ . (a, c, and e), the plots with gravel-sand mulching; (b, d, and f), the plots without gravel-sand mulching.

of soil water at the soil depth of 0–30 cm changed most significantly ( $P<0.05$ ) (the plots without gravel-sand mulching:  $\delta^2\text{H}$ ,  $-83.47\text{‰}$ – $-30.27\text{‰}$ ;  $\delta^{18}\text{O}$ ,  $-11.96\text{‰}$ – $-2.32\text{‰}$ ; the plots with gravel-sand mulching:  $\delta^2\text{H}$ ,  $-85.13\text{‰}$ – $-53.34\text{‰}$ ;  $\delta^{18}\text{O}$ ,  $-12.10\text{‰}$ – $-6.34\text{‰}$ ). Moreover, the stable isotopes values of soil water at the soil depth of 0–30 cm were significantly richer than those at the soil depth of 30–150 cm, which is mainly due to the influence of evaporation. However, the stable isotopes enrichment of deep soil water in plot C and plot D was not affected by evaporation, which may be caused by the infiltration of enriched soil water in the surface layer. In terms of sampling time, there were some differences in the average stable isotopes values of each month, but there was no regular change with the sampling time. The monthly variation in the stable isotopes values of soil water in the plots without gravel-sand mulching ( $\delta^2\text{H}$ ,  $2.33\text{‰/month}$ – $6.37\text{‰/month}$ ;  $\delta^{18}\text{O}$ ,  $0.15\text{‰/month}$ – $0.87\text{‰/month}$ ) was greater than that in the plots with gravel-sand mulching ( $\delta^2\text{H}$ ,  $1.89\text{‰/month}$ – $3.89\text{‰/month}$ ;  $\delta^{18}\text{O}$ ,  $0.19\text{‰/month}$ – $0.59\text{‰/month}$ ). The result was almost consistent with the monthly change of the soil water content, which indicated that gravel-sand mulching weakens the intensity of soil water evaporation. The depletion and enrichment of  $\delta^2\text{H}$  and  $\delta^{18}\text{O}$  were the results of evaporation, and the stable isotopes values in the plots with gravel-sand mulching were lower than those in the plots without gravel-sand mulching. Therefore, the change of the stable isotopes values of soil water is a good indication of soil evaporation under different mulching measures.

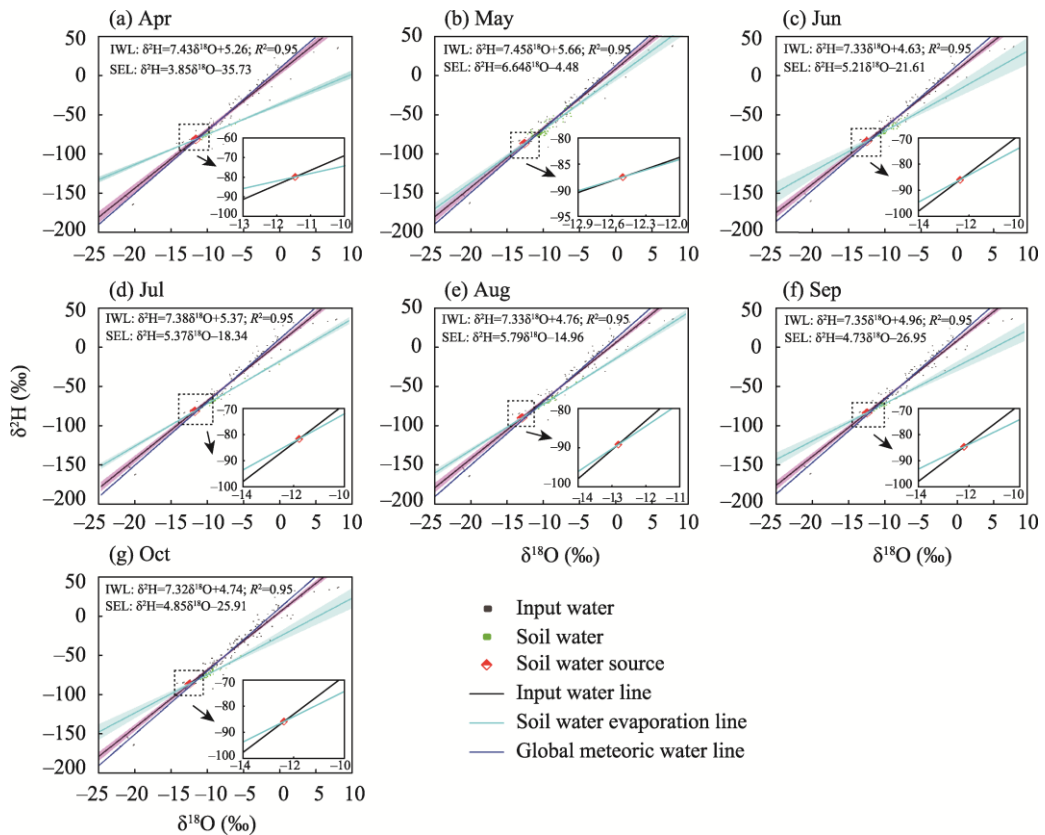


**Fig. 4** Input water line, soil water evaporation line, and global meteoric water line in April (a), May (b), June (c), July (d), August (e), September (f), and October (g). The shaded areas are 95% confidence interval.

### 3.3 Soil evaporation loss rate

The evaporation fractionation signals of soil water stable isotopes at the soil depth of 0–30 cm were well preserved, so we discussed the monthly soil evaporation loss rate at this depth. We used the lc-excess value to express the deviation degree of the stable isotopes values of soil

water from the input water line; the smaller the value is, the stronger the evaporation fractionation is (Table 2). In terms of spatial variation, with the increase of soil depth, the lc-excess values of the plots with and without gravel-sand mulching showed an increasing trend, indicating that the closer to the surface, the stronger the evaporation. In terms of temporal variation, the trend of lc-excess value was nearly consistent with the change of the stable isotopes values of soil water. The average lc-excess value of the plots with gravel-sand mulching was  $-4.86\text{‰}$ , and the average lc-excess value of the plots without gravel-sand mulching was  $-7.79\text{‰}$ . Obviously, the gravel-sand mulching measure weakens the evaporation of soil water.

**Table 2** Line-conditioned excess (lc-excess) values of the plots with and without gravel-sand mulching at the soil depth of 0–30 cm

Plot	Soil depth (cm)	Lc-excess (‰)						
		Apr	May	Jun	Jul	Aug	Sep	Oct
A	0–10	−14.68	−1.23	−10.87	−9.97	−8.11	−2.97	−4.84
	10–20	−7.43	−5.24	−2.84	−6.04	−5.13	−1.17	−3.55
	20–30	−5.74	−0.37	−3.67	−3.21	−4.04	−4.47	−4.85
C	0–10	−16.34	−6.74	−7.33	−7.51	−5.54	−3.16	−4.64
	10–20	−6.95	−8.15	−2.01	−3.26	−0.70	−2.95	−5.74
	20–30	−4.73	−9.72	−0.87	−1.73	−1.57	−0.51	−5.27
E	0–10	−18.28	−1.74	−10.82	−9.63	−6.29	−8.26	−9.76
	10–20	−9.90	−1.87	−5.16	−7.73	−4.15	−4.85	−3.39
	20–30	−4.86	−3.56	−1.77	−6.94	−4.19	−3.13	−4.09
B	0–10	−17.93	−1.61	−17.50	−13.39	−13.62	−5.75	−5.53
	10–20	−6.39	−9.73	−3.66	−6.67	−8.10	−4.30	−5.35
	20–30	−1.24	−3.34	−1.82	−4.99	−7.45	−4.46	−6.92
D	0–10	−12.37	−8.11	−31.21	−12.51	−9.35	−6.21	−5.20
	10–20	−3.03	−8.94	−12.34	−5.50	−8.21	−3.65	−4.37
	20–30	−2.64	−5.94	−8.29	−3.55	−6.54	−2.33	−6.43
F	0–10	−13.67	−0.63	−26.53	−18.53	−7.83	−11.99	−10.99
	10–20	−5.64	−0.01	−8.92	−9.43	−4.30	−8.20	−9.08
	20–30	−4.85	−0.10	−5.63	−9.50	−5.37	−3.39	−9.58

Note: A, C, and E are the plots with gravel-sand mulching; B, D, and F are the plots without gravel-sand mulching.

Figure 5 showed that, whether the soil is mulched with gravel and sand or not, evaporation was the strongest in April (the soil evaporation loss rate calculated by  $\delta^2\text{H}$  using Craig-Gordon model ( $f_{\text{H}}^2$ ), 35.03%; the soil evaporation loss rate calculated by  $\delta^{18}\text{O}$  using Craig-Gordon model ( $f_{\text{O}}^{18}$ ), 37.58%; and the soil evaporation loss rate calculated by the lc-excess coupled Rayleigh fractionation model ( $f_{\text{lc-excess}}$ ), 58.31%) and relatively weak in May ( $f_{\text{H}}^2$ , 12.34%;  $f_{\text{O}}^{18}$ , 22.07%; and  $f_{\text{lc-excess}}$ , 33.09%) and September ( $f_{\text{H}}^2$ , 10.73%;  $f_{\text{O}}^{18}$ , 16.37%; and  $f_{\text{lc-excess}}$ , 30.83%). In the growing season of peach trees, the average soil evaporation loss rate in the plots with gravel-sand mulching was 11.54% for  $f_{\text{H}}^2$ , 17.19% for  $f_{\text{O}}^{18}$ , and 29.52% for  $f_{\text{lc-excess}}$ , and the average soil evaporation loss rate in the plots without gravel-sand mulching was 21.69% ( $f_{\text{H}}^2$ ), 27.96% ( $f_{\text{O}}^{18}$ ), and 43.94% ( $f_{\text{lc-excess}}$ ). Obviously, gravel-sand mulching reduces the consumption of ineffective water. The difference in the soil evaporation loss rate between the plots with and without gravel-sand mulching was the largest in August, which indicated that the effect of gravel-sand mulching measures is most prominent in August, so we can increase the thickness of gravel-sand mulching in this month.

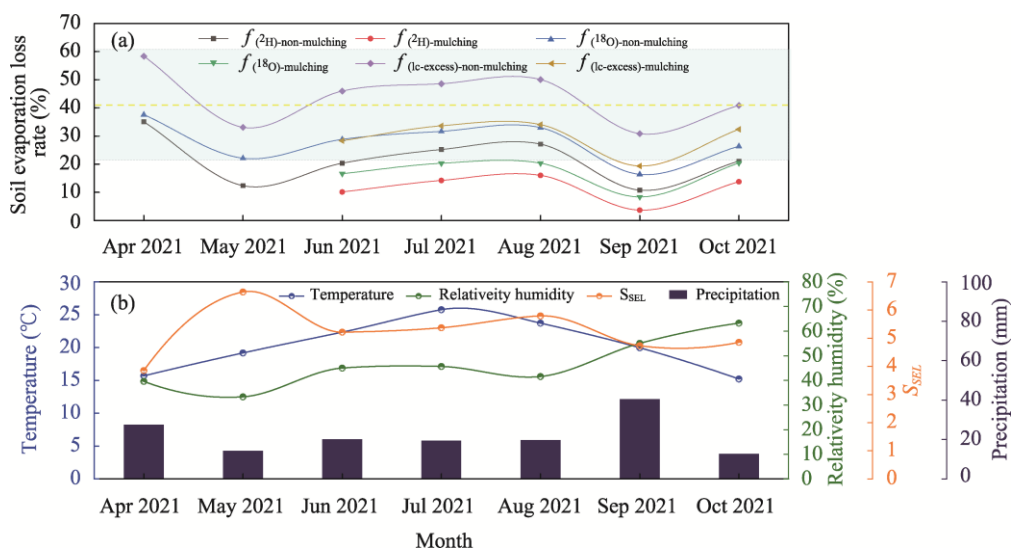


**Fig. 5** Temporal variation of the soil evaporation loss rate (a), temperature, relative humidity, soil evaporation line slope ( $S_{SEL}$ ), and precipitation (b).  $f^{(2H)}$ , the soil evaporation loss rate calculated by  $\delta^2H$  using Craig-Gordon model;  $f^{(18O)}$ , the soil evaporation loss rate calculated by  $\delta^{18O}$  using Craig-Gordon model;  $f_{(lc-excess)}$ , the soil evaporation loss rate calculated by line-conditioned excess coupled Rayleigh fractionation model; the subscripts of mulching and non-mulching represent the plots with and without gravel-sand mulching, respectively. The shaded area is the soil evaporation loss rate in similar environments, and the yellow dashed line is the average soil evaporation loss rate in similar environments (Schlesinger and Jasechko, 2014).

## 4 Discussion

### 4.1 Influencing factors of soil evaporation

We applied the lc-excess value to qualitatively determine the intensity of soil evaporation, and used the lc-excess coupled Rayleigh fractionation model and Craig-Gordon model to quantitatively calculate the soil evaporation loss rate. However, soil evaporation is the result of many factors. The lc-excess value includes many other factors that affect soil evaporation when it expresses the intensity of evaporative fractionation, therefore, we analyze the correlation between lc-excess value and other factors (Table 1). The lc-excess value was positively correlated with relative humidity, with a correlation coefficient of 0.50, and negatively correlated with average temperature, with a correlation coefficient of  $-0.48$ ; and the correlation coefficients of lc-excess value with input water content and the soil water content were 0.61 and 0.87, respectively. The lc-excess value can reflect the strength of evaporation. The results showed that evaporation is stronger in April, which may be because the branches and leaves of the peach trees are not fully developed at the early stage of growth. Therefore, we performed a correlation analysis between crown width and evaporation, and the average correlation coefficient was 0.70 ( $P < 0.01$ ; Table 1). In other words, lush branches and leaves can reduce the evaporation of soil water to a certain extent. The relatively weak evaporation in May and September is not affected by crown width, which may be attributed to the amount of water input (Hasselquist et al., 2018; Dubbert et al., 2019). There is a negative correlation between evaporation and input water content, and the average correlation coefficient is  $-0.51$  ( $P < 0.05$ ; Table 1). Due to the existence of irrigation in early May, the total water input in May is larger than that in September, so the soil evaporation loss rate in May is slightly smaller than that in September. The average correlation coefficients of evaporation with relative humidity, average temperature, and soil water content were  $-0.71$ , 0.55, and  $-0.73$ , respectively ( $P < 0.01$ ; Table 1). The soil evaporation loss rate is negatively correlated with relative humidity and positively correlated with average temperature, which is consistent with the fact that evaporation will be weaker with higher humidity and stronger with higher

temperature. These findings are consistent with the research results of Xiang et al. (2021), which showed that soil evaporation is affected by multiple factors.

## 4.2 Calculation of the soil evaporation loss rate

Soil evaporation will cause water isotopes fractionation, resulting in changes of soil water stable isotopes values (Zimmermann et al., 1966; Allison and Barnes 1983). Therefore, the influence of soil evaporation can be explored through the changes of soil water stable isotopes values (Sprenger et al., 2017). However, it is generally believed that the direct evaporation depth can occur only at the top of soil layer (Or et al., 2013; Piri et al., 2020), but some studies showed that the fractionation signal of isotopes can reach the soil depth of 20–30 cm in temperate regions, and it can reach the soil depth of 50 cm in Mediterranean climate regions (Sprenger et al., 2016). In this study, the fractionation signals of soil water isotopes at the soil depth of 0–30 cm are prominent, so we calculated the soil evaporation loss rate at this depth.

There are two methods to calculate the proportion of water entering the soil returning to the atmosphere through soil evaporation (i.e., the soil evaporative loss rate). The first method is based on the Rayleigh fractionation (Clark and Fritz, 1997), and the second method is based on the Craig-Gordon model (Gonfiantini, 1986; Sprenger et al., 2017). To highlight the isotopic advantage, we used the lc-excess coupled Rayleigh fractionation model in this study. In general, plot A and plot B in the lc-excess coupled Rayleigh fractionation model represent the slope and intercept of the local precipitation line, respectively. Since there is irrigation in these plots, we fitted the input water line of each month, and the lc-excess value represents the deviation degree of isotopes value in the sample from the input water line, which makes the lc-excess coupled Rayleigh fractionation model more accurate. When the Craig-Gordon model is applied to calculate the soil evaporation loss rate, the soil water source needs to be determined, which is usually determined by the soil evaporation line and local meteoric water line, and the intersection of the two is the soil water source (Javaux et al., 2016). Most studies only identified one soil water source to calculate the soil evaporation loss rate in time series (Gibson et al., 2016; Che et al., 2020; Mahindawansa et al., 2020), ignoring the input of precipitation and irrigation water. For this reason, we determined the soil water source of each month through the input water line and soil evaporation line of each month (Fig. 4 and Table 3), which can improve the computational accuracy of the Craig-Gordon model to a certain extent.

**Table 3** Soil water source during April–October in 2021

Month	Soil water source	
	$\delta^{18}\text{O}$ (‰)	$\delta^2\text{H}$ (‰)
April 2021	−11.45	−79.86
May 2021	−12.50	−87.47
June 2021	−12.35	−85.99
July 2021	−11.79	−81.65
August 2021	−12.81	−89.20
September 2021	−12.20	−84.67
October 2021	−12.39	−85.92

We calculated the soil evaporation loss rate at the soil depth of 0–30 cm by the lc-excess coupled Rayleigh fractionation model and Craig-Gordon model. The change trends of  $f_{(\text{lc-excess})}$ ,  $f_{(^{18}\text{O})}$ , and  $f_{(^2\text{H})}$  with time are consistent, and the correlation coefficient of the lc-excess value with  $f_{(\text{lc-excess})}$ ,  $f_{(^{18}\text{O})}$ , and  $f_{(^2\text{H})}$  are −0.62, −0.56, and −0.48, respectively. Then, we compared the soil evaporation loss rate in similar environments (Fig. 5), and found that  $f_{(\text{lc-excess})}$  is completely located in the shaded area, followed by  $f_{(^{18}\text{O})}$ , which is consistent with the correlation between evaporation and the lc-excess value. The relatively poor calculation result of  $f_{(^2\text{H})}$  may be because  $^2\text{H}$  is more affected by artificial intervention such as fertilization in cultivated soil, while  $^{18}\text{O}$  is less affected by artificial intervention. Moreover, when the lc-excess value was used to calculate

evaporation, the influence of  $^2\text{H}$  and  $^{18}\text{O}$  was weakened, so  $f_{(\text{lc-excess})}$  achieved the best result, followed by  $f(^{18}\text{O})$ .

### 4.3 Effects of gravel-sand mulching on soil evaporation

We compared the difference of the soil evaporation loss rate at the soil depth of 0–30 cm. Throughout the growing season, the evaporation of soil water in the plots with gravel-sand mulching was significantly lower than that in the plots without gravel-sand mulching. In addition, the soil water content in the plots with gravel-sand mulching was also higher than that in the plots without gravel-sand mulching. The difference of the soil evaporation loss rate caused by gravel-sand mulching is the largest in August; that is, the effect of gravel-sand mulching on inhibiting soil evaporation is most prominent in August.

Gravel-sand mulching is the main reason for the difference of soil water evaporation signals. Surface mulching changes the amount of water and heat exchange between the Earth and atmosphere, affecting the soil water phase transition (Fu et al., 2015), soil water and heat transfer (Lu et al., 2019), and soil water evaporation (Chen et al., 2019). In agriculture, gravel-sand mulching is often used to reduce the ineffective evaporation of soil water during crop growth season (Tan et al., 2019). This approach is used because the surface mulched with gravel and sand can cut off the rising path of the lower soil moisture and change the position of the evaporation interface, so that the rising soil moisture is stored near the surface and any water vapor must pass through the sand layer to escape into the atmosphere. Gravel-sand mulching avoids partial soil water loss due to evaporation and reduces the soil evaporation loss rate. The study of farmland water status under the condition of gravel-sand mulching will be helpful to guide production practices and further improve the basic theory of mulching technology in agricultural water-saving to alleviate the substantial pressure caused by the shortage of water resources in Northwest China, which has important scientific value and practical significance for guiding the efficient utilization of agricultural water resources. Therefore, we suggest to implement gravel-sand mulching measures in the crops growing season in water-deficient areas, and appropriately increase the thickness of gravel-sand mulching in July and August to achieve better water retention.

## 5 Conclusions

We monitored the variation characteristics of soil water content and stable isotopes values during the growth season of Baifeng peach (*Amygdalus persica* L.) in 2021 and analyzed the characteristics of soil water and the soil evaporative loss rate when mulched with and without gravel and sand. Our results showed that the average soil water content in the plots with gravel-sand mulching is 1.86% higher than that without gravel-sand mulching, and the monthly variation of the soil water content is smaller in the plots with gravel-sand mulching than that in the plots without gravel-sand mulching. Second, the lc-excess value was negative for both the plots with and without gravel-sand mulching. The average lc-excess value of the plots without gravel-sand mulching is 2.93% lower than that of the plots with gravel-sand mulching. The lc-excess value has good correlation with relative humidity, average temperature, input water content, and soil water content. The difference of the soil evaporation loss rate between the plots with and without gravel-sand mulching is the largest in August, and the inhibition effect of gravel-sand mulching on soil evaporation is most prominent in August. In conclusion, we quantified the influence of gravel-sand mulching on the soil water content and soil evaporation loss rate in this study, which provides some basic data support for improving water use efficiency and saving water resources.

## Acknowledgements

This study was supported by the National Natural Science Foundation of China (41771035, 42071047). The authors are very grateful to the colleagues at the Northwest Normal University for their help in field work, laboratory analysis, and data processing.

## References

- Allison G B, Barnes C J. 1983. Estimation of evaporation from non-vegetated surfaces using natural deuterium. *Nature*, 301(5896): 143–145.
- Al-Oqaili F, Good S P, Peters R T, et al. 2020. Using stable water isotopes to assess the influence of irrigation structural configurations on evaporation losses in semiarid agricultural systems. *Agricultural and Forest Meteorology*, 291: 108083, doi: 10.1016/j.agrformet.2020.108083.
- Barnes C J, Allison G B. 1984. The distribution of deuterium and  $^{18}\text{O}$  in dry soils: 3. Theory for non-isothermal water movement. *Journal of Hydrology*, 74(1–2): 119–135.
- Benettin P, Volkmann T H, Freyberg J V, et al. 2018. Effects of climatic seasonality on the isotopic composition of evaporating soil waters. *Hydrology and Earth System Sciences*, 22(5): 2881–2890.
- Che C W, Zhang M J, Wang S J, et al. 2020. Studying spatio-temporal variation and influencing factors of soil evaporation in southern and northern mountains of Lanzhou city based on stable hydrogen and oxygen isotopes. *Geographical Research*, 39(11): 2537–2551. (in Chinese)
- Chen F L, Zhang M J, Ma Q, et al. 2013. Characteristics of  $\delta^{18}\text{O}$  in precipitation and water vapor sources in Lanzhou City and its surrounding area. *Environmental Science*, 34(10): 3755–3763. (in Chinese)
- Chen J, Xie X, Zheng X, et al. 2019. Effect of straw mulch on soil evaporation during freeze-thaw periods. *Water*, 11(8): 1689, doi: 10.3390/w11081689.
- Clark I D, Fritz P. 2013. *Environmental Isotopes in Hydrogeology*. Boca Raton: CRC Press.
- Craig H, Gordon L I. 1965. Deuterium and oxygen-18 variations in the ocean and the marine atmosphere. In: *Proceedings of a Conference on Stable Isotopes in Oceanographic Studies and Palaeo Temperatures*. Pisa, Italy.
- Dang Y. 2004. The environmental degeneration has influence on the climate of Lanzhou area. *Journal of Northwest University (Natural Science Edition)*, 34(3): 355–358. (in Chinese)
- Dubbert M, Caldeira M C, Dubbert D, et al. 2019. A pool-weighted perspective on the two-water-worlds hypothesis. *New Phytologist*, 222(3): 1271–1283.
- Fu Q, Li T N, Li T X, et al. 2015. Influence of straw mulching on soil moisture characteristics during seasonal freeze-thaw period. *Transactions of the Chinese Society for Agricultural Machinery*, 46(6): 141–146. (in Chinese)
- Gibson J J, Birks S J, Edwards T W D. 2008. Global prediction of  $\delta_A$  and  $\delta^2\text{H}-\delta^{18}\text{O}$  evaporation slopes for lakes and soil water accounting for seasonality. *Global Biogeochemical Cycles*, 22(2): GB2031, doi: 10.1029/2007GB002997.
- Gibson J J, Reid R. 2014. Water balance along a chain of tundra lakes: A 20-year isotopic perspective. *Journal of Hydrology*, 519: 2148–2164.
- Gibson J J, Birks S J, Yi Y. 2016. Stable isotope mass balance of lakes: a contemporary perspective. *Quaternary Science Reviews*, 131: 316–328.
- Gonfiantini R. 1986. Environmental isotopes in lake studies. *The Terrestrial Environment*, B, 2: 113–168.
- Hasselquist N J, Benegas L, Rupsard O, et al. 2018. Canopy cover effects on local soil water dynamics in a tropical agroforestry system: Evaporation drives soil water isotopic enrichment. *Hydrological Processes*, 32(8): 994–1004.
- Horita J, Wesolowski D J. 1994. Liquid-vapor fractionation of oxygen and hydrogen isotopes of water from the freezing to the critical temperature. *Geochimica et Cosmochimica Acta*, 58(16): 3425–3437.
- Horita J, Rozanski K, Cohen S. 2008. Isotope effects in the evaporation of water: a status report of the Craig-Gordon model. *Isotopes in Environmental and Health Studies*, 44(1): 23–49.
- Hsieh J C, Chadwick O A, Kelly E F, et al. 1998. Oxygen isotopic composition of soil water: quantifying evaporation and transpiration. *Geoderma*, 82(1–3): 269–293.
- Hu Y, Liu Z, Zhao M, et al. 2018. Using deuterium excess, precipitation and runoff data to determine evaporation and transpiration: A case study from the Shawan Test Site, Puding, Guizhou, China. *Geochimica et Cosmochimica Acta*, 242: 21–33.
- Javaux M, Rothfuss Y, Vanderborght J, et al. 2016. Isotopic composition of plant water sources. *Nature*, 536(7617): E1–E3.
- Kang S Z. 2019. National water conservation initiative for promoting water-adapted and green agriculture and highly-efficient water use. *China Water Resources*, (13): 1–6. (in Chinese)
- Kool D, Agam N, Lazarovitch N, et al. 2014. A review of approaches for evapotranspiration partitioning. *Agricultural and Forest Meteorology*, 184: 56–70.
- Landwehr J M, Coplen T B. 2006. Line-conditioned excess: a new method for characterizing stable hydrogen and oxygen isotope ratios in hydrologic systems. In: *International Conference on Isotopes in Environmental Studies*. Vienna, Austria.
- Lu X, Li R, Shi H, et al. 2019. Successive simulations of soil water-heat-salt transport in one whole year of agriculture after

- different mulching treatments and autumn irrigation. *Geoderma*, 344: 99–107.
- Mahindawansa A, Külls C, Kraft P, et al. 2020. Investigating unproductive water losses from irrigated agricultural crops in the humid tropics through analyses of stable isotopes of water. *Hydrology and Earth System Sciences*, 24(7): 3627–3642.
- Merlivat L. 1978. The dependence of bulk evaporation coefficients on air-water interfacial conditions as determined by the isotopic method. *Journal of Geophysical Research: Oceans*, 83(C6): 2977–2980.
- Or D, Lehmann P, Shahraeeni E, et al. 2013. Advances in soil evaporation physics—A review. *Vadose Zone Journal*, 12(4): 1–16.
- Piri J, Malik A, Kisi O. 2020. Assessment and simulation of evaporation front depth and intensity from different soil surface conditions regarding diverse static levels. *Water Productivity Journal*, 1(1): 1–20.
- Poesen J, Van Wesemael B, Govers G, et al. 1997. Patterns of rock fragment cover generated by tillage erosion. *Geomorphology*, 18(3–4): 183–197.
- Schlesinger W H, Jasechko S. 2014. Transpiration in the global water cycle. *Agricultural and Forest Meteorology*, 189: 115–117.
- Sprenger M, Leistert H, Gimbel K, et al. 2016. Illuminating hydrological processes at the soil-vegetation-atmosphere interface with water stable isotopes. *Reviews of Geophysics*, 54(3): 674–704.
- Sprenger M, Tetzlaff D, Soulsby C. 2017. Soil water stable isotopes reveal evaporation dynamics at the soil-plant-atmosphere interface of the critical zone. *Hydrology and Earth System Sciences*, 21(7): 3839–3858.
- Tan J L, Wang X N, Tian J C, et al. 2017. Water retention characteristics of gravel-sand stratum on the gravel-sand mulched field. *Chinese Journal of Soil Science*, 48(2): 319–325. (in Chinese)
- Xiang W, Si B C, Li M, et al. 2021. Stable isotopes of deep soil water retain long-term evaporation loss on China's Loess Plateau. *Science of the Total Environment*, 784: 147153, doi: 10.1016/j.scitotenv.2021.147153.
- Yuan C F, Feng S Y, Huo Z L, et al. 2019. Effects of deficit irrigation with saline water on soil water-salt distribution and water use efficiency of maize for seed production in arid Northwest China. *Agricultural Water management*, 212: 424–432.
- Zhao W J, Yu P, Ma X Y, et al. 2017. Numerical simulation of soil evaporation with sand mulching and inclusion. *Water*, 9(4): 294, doi: 10.3390/w9040294.
- Zimmermann U, Münnich K O, Roether W, et al. 1966. Tracers determine movement of soil moisture and evapotranspiration. *Science*, 152(3720): 346–347.